Available online at www.worldscientificnews.com

World Scientific News

An International Scientific Journal

WSN 142 (2020) 76-87 EISSN 2392-2192

Spatial and temporal patterns of ocean variability using empirical orthogonal functions (EOF) in the Southern Java Waters

Mega Syamsuddin

Department of Marine Science, Faculty of Fisheries and Marine Sciences, Universitas Padjadjaran, Jalan Raya Bandung-Sumedang KM 21 Jatinangor, Sumedang, Indonesia

E-mail address: vegha16@gmail.com

ABSTRACT

The oceanographic parameters of Sea Surface Temperature (SST) from NOAA/AVHRR, Chlorophyll-*a* (Chl-*a*) from SeaWiFS and Modis/Aqua, Sea Surface Height Anomaly (SSHA) and eddy kinetic energy (EKE) from from TOPEX and Poseidon ERS-1/2 are used to understand the oceanographic variability in the Southern Java Waters. Analyses were done using empirical orthogonal function (EOF) and wavelet spectrum analysis in order to know spatial and temporal distributions related to the main forcing of the ocean climate variability for the period of January 1997 to December 2008 (12 years). The first EOF modes of Chl-*a*, SSHA and SST accounted for 42.8%, 36.5%, and 27.4% of total variance, corresponded with interannual signal for all the first modes, respectively. The spatial patterns of the first and second EOF modes of SSHA, SST and Chl-*a* gave a very typical cold water of SSHA, low SST and high Chl-*a* concentration located along the southern coast of Indonesian archipelago and warm water of SSHA, high SST and much less Chl-*a* concentration in the offshore region to make frontal areas along the latitudinal line around 10–12ºS. The results showed that total variance of the first two mode of SSHA, SST, and Chl-*a* explain 59.94%, 35.52%, and 55.26 %, respectively. These infer that SSHA and Chl-*a* give more response to the climate variability of El Niño Southern Oscillation (ENSO) forcing in the study area.

***Keywords*:** El Niño Southern Oscillation, Empirical Orthogonal Function, Ocean variability

(Received 23 January 2020; Accepted 10 February 2020; Date of Publication 11 February 2020)

1. INTRODUCTION

The southern Java are located at low latitudes between the Indian and Pacific Oceans, the only connection between ocean basins at low latitudes at which interocean exchange can occur [1]. This connection permits the transfer of Pacific waters into the Indian Ocean. As a result, the Indonesian Through Flow (ITF) plays an important role in climate system [2]. Due to its unique geographic position, the weather and oceanographic conditions in the Southern Java waters to be affected directly by regional climate change of El Niño Southern Oscillation (ENSO) and Indian Ocean Dipole (IOD) being the dominant forcing mechanism in this region [3].

The region is rich with sources of interannual, seasonal, intraseasonal ocean variations that have direct impacts on the environmental conditions in the Southern Java Waters. Previous studies showed that the current and wave dynamics are affected directly by the variability of ENSO as well as the monsoon system [4]. Interannual signals in the ITF therefore forced by interannual variability associated with ENSO as well as by the IOD [5]

The ENSO and IOD are two dominant modes of climate variations in the tropical Pacific and Indian Oceans, respectively. Both modes are two obvious drivers of climate with significant impacts to the ocean climate variability of several parts of the world [6]. The ENSO cycle is the largest known source of year-to-year climate variability. Climate variability refers to the variations in the mean state of the climate (on all spatial and temporal scales) beyond that of individual weather events. Climate plays a large role in determining short-term, seasonal and multi-year patterns of variability in the location and productivity of the optimal tuna habitat zones.

Besides ENSO and IOD, in a shorter timescale, winds over the Indonesian maritime continent have a strong monsoonal signal. The winds over the Indonesia maritime continent and the position of the Inter Tropical Convergence Zones (ITCZ) cause a strong monsoonal system where during the southeast (SE) monsoon (April to September), southeasterly wind from Australia generates upwelling and reversed condition occurs during the northwest (NW) monsoon (October to March) with down welling along southern coast of Indonesian archipelago [2].

Upwelling as characterized by low sea surface temperature below 28 ºC [7] together with the confluence of ITF, SJC, SEC, and RWs make the regions very dynamic. Therefore the objective of this research is to examine the most dominat forcing on the variability of oceanographic conditions in the Southern Java.

2. MATERIALS AND METHODS

2. 1. Study area

The study area was located in the eastern Indian Ocean, south of Java, spanning 6–16° S and 104–126° E (Figure 1). The Indonesian seas are the only major low-latitude connection in the global oceans. This connection permits the transfer of Pacific waters into the Indian Ocean [8]. The Indonesian water is exported into the Indian Ocean within three major passages: Timor passage, Ombai Strait and Lombok Strait, the waters of the ITF are apparent within the thermocline as a relatively cool and low salinity.

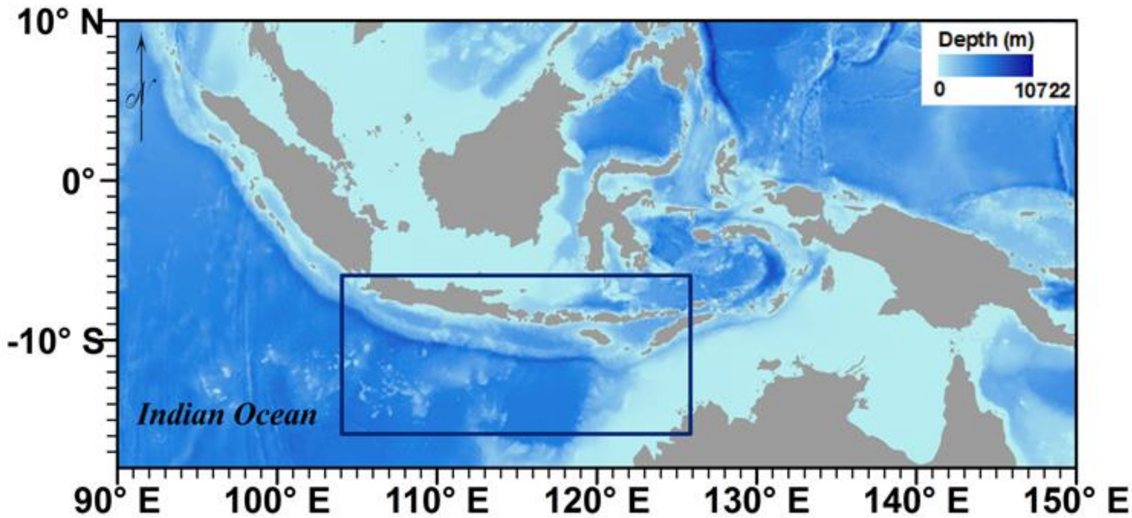

Figure 1. Map of the Indonesian Seas with the inset box representing the study area in the Southern Java Sea

2. 2. Data

In this study, the satellite remotely sensed data were analyzed for the 12 years datasets from January 1997-December 2008 and emphasized the differences of regional climate conditions during strong (1997), moderate (2002), and weak (2006) El Niño, moderate (2003) positive phase of IOD, strong (1999) La Niña, and normal year (2005) events. All the data used in this study are summarized in Table 1.

Table 1. A description of satellite data and in situ data used in this study.

Data	Spatial resolution	Temporal resolution
Remotely sensed: SSHA (AVISO) EKE (AVISO) SST (NOAA/AVHRR) Chl-*a* (SeaWiFS and Modis/Aqua)	 1/3° 1/3° 4 km 9 km	Monthly
Climatic indices: Niño 3.4 Index Dipole Mode Index		 Monthly Monthly

The SSHA, SST and EKE images are matched with the temporal scale for Chl-*a* which have 9 km resolution. The SSHA data derived from the TOPEX and Poseidon ERS-1/2 altimeters which are produced and distributed by Archived Validation and Interpretation of Satellite Oceanographic Data (AVISO). The monthly mean of SSHA calculated from 7 day composite cycles of SSHA products. The SSHA data have a spatial resolution 1/3° and were resampled to 9 km resolution.

As for the EKE, the weekly global geostrophic current velocity images from AVISO were averaged into monthly data for the u and v components with the spatial resolution of 1/3°. The u and v rasters were used to calculate the EKE using the equation introduced by Robinson (2004) as shown below:

$$EKE = 1/2\ (u^2 + v^2) \quad (1)$$

SST data were derived from the Advanced Very High Resolution Radiometer (AVHRR) sensor on board the National Oceanic and Atmospheric Administration (NOAA) satellite. The dataset is distributed by the Physical Oceanography Distributed Active Archive Center (PODAAC: http://podaac.jpl.nasa.gov) of the Jet Propulsion Laboratory (JPL)/National Aeronautics and Space Administration (NASA). The monthly mean SST dataset at a pixel resolution of 4 × 4 km then resampled to 9 km.

Chl-*a* data were derived from SeaWiFS Level 3 images at a spatial resolution of 9 × 9 km. Monthly composite data were downloaded from http://oceancolor.gsfc.nasa.gov. These data were processed using the SeaWiFS Data Analysis System (SeaDAS VA 6.1) provided by The National Aeronautics and Space Administration (NASA).

For data analysis, all SSHA, SST, Chl-*a* and EKE were composed into monthly data using SeaDAS VA 6.1 and resampled into 9 km spatial resolution. The 9-km-resolution data were used to capture dynamic features of the oceanographic conditions that represented El Niño, positive phase of IOD and La Niña events.

The Niño 3.4 and Dipole Mode indices were used as proxy to climatic conditions of ENSO and IOD, respectively. The Niño 3.4 index is the averaged SST anomalies in the region bounded by 5° N - 5° S, from 120° - 170° W. This region has large variability on El Niño time scales, and close to the region where changes in local SST are important for shifting the large region of rainfall typically located in the far western Pacific. The index is available at the NOAA Climate Prediction Center (http://www.cpc.ncep.noaa.gov).

El Niño and La Niña events have been identified if the 5 month running average of the Niño 3.4 index exceeds +0.5 °C for El Niño and -0.5 °C for La Niña for at least 5 consecutive months. Intensity of the IOD is represented by Dipole Mode Index (DMI) which is anomalous SST gradient between the western equatorial Indian Ocean (50-70 °E and 10 °S - 10 °N) and the south eastern equatorial Indian Ocean (90-110 °E and 10 °S - 0 °N).

The index is available at the Japan Agency for Marine-Earth Science and Technology/JAMSTEC (www.jamstec.go.jp). When the DMI is positive (negative), the phenomenon is referred as the positive (negative) IOD which indicates dry (wet) impacts similar to El Niño (La Niña) in the Pacific Ocean (Figure 2).

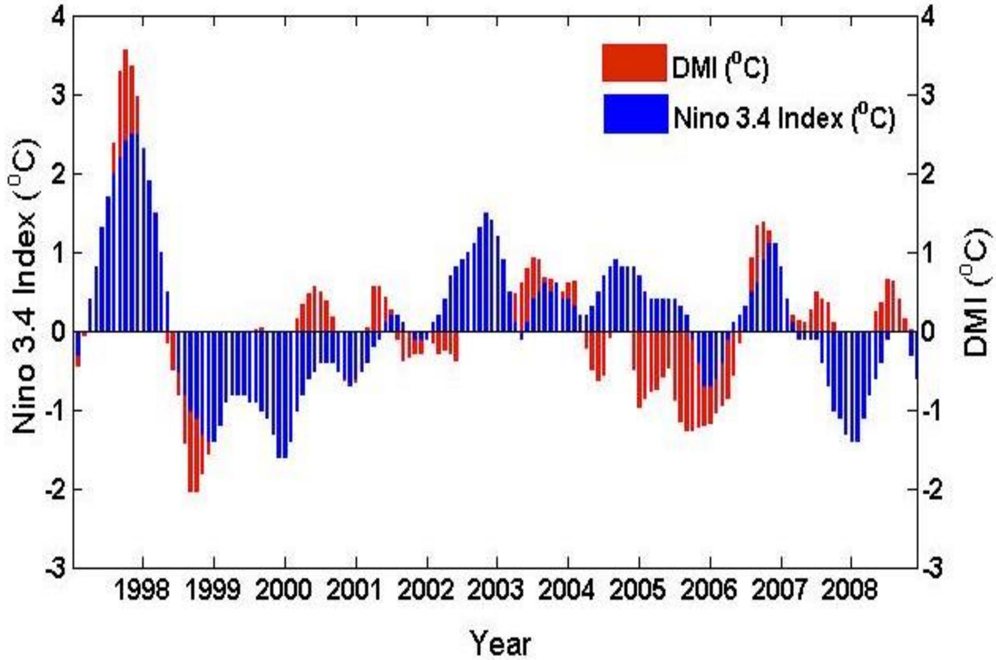

Figure 2. SST anomalies from the Niño 3.4 index (blue bars) and Dipole Mode Index (red bars) during January 1997-December 2008.

2. 3. Methods: Statistical analysis

2. 3. 1 Empirical orthogonal function

This study applied the empirical orthogonal function (EOF) analysis as a statistical method to quantitatively examine oceanographic parameters. EOF analysis is a useful technique for decomposition of a time series of geophysical data into temporal and spatial variability in terms of orthogonal functions, or statistical modes. EOF analysis has been used commonly to describe spatial-temporal ocean variability [9]. EOF analysis was applied to the raw weekly dataset of SSHA and SST and monthly data of Chl-*a* (because of a lack of data in many of the weekly images) in order to decompose the total variability into major modes associated with interannual and seasonal variability. Here, I examined only the first and second dominant modes, which were statistically independent and significant which are statistically independent and significant [10]. Eigenvalues with contribution rates over 5% are considered significant for the 95% confidence limit.

The first standard procedure in the EOF analysis is to subtract a long-term mean from each of the SSHA, SST and Chl-*a* time series data, and then to set up the matrix F that consists of row (temporal dataset) and columns (spatial dataset) vectors.

2. 3. 2. Wavelet spectrum analysis

In this study, the continous wavelet transform (CWT) analysis was applied on the monthly of SST, SSHA, and Chl-*a* data. The wavelet transform analysis (WT) was performed to obtain the temporal distributions the ocean variability during 1997-2008. Wavelet analysis performs a time frequency analysis of the dominant signal and decompose the signal in different time scales and identify how these signals vary in time. The wavelet transform has been successfully applied in climate studies [11]. High energy variances are represented in red and low values are in blue as shown in the colorbars that represent different wavelet amplitude. The black line (solid contour) shows the 95% confidence level and a thin black line shows the cone of influence (COI) [12].

3. RESULT AND DISCUSSION

3. 1. Climate feature of oceanographic conditions

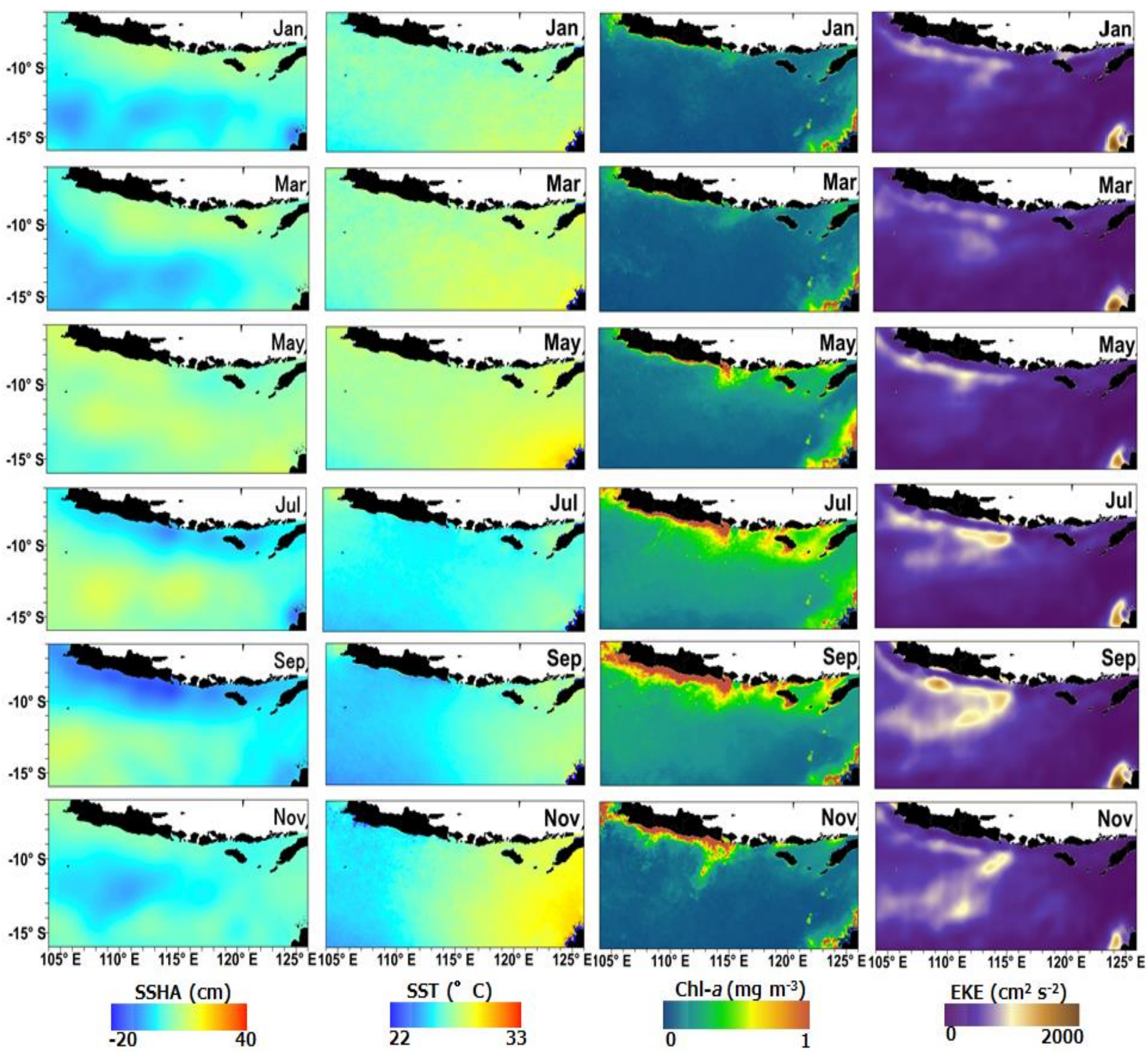

Figure 3. Climatological monthly composite of SSHA, SST, Chl-*a* and EKE from 1997 to 2008 in the Southern Java waters. Scale units are in centimeters, degrees Celcius, and milligrams per cubic meter, and centimeters square per second square for SSHA, SST, Chl-*a*, and EKE data, respectively.

The patterns of the climatological annual cycle of SSHA, SST, Chl-*a* concentration and EKE during 1997-2008 in the Southern Java showed in Figure 3. There is a clear seasonal dependence of all oceanographic parameter (SSHA, SST, Chl-*a* and EKE) with the southeast monsoon (SE) show a stronger impact to cause negative SSHA from -1 to -20 cm following by colder water of SST (24-27 ºC) and high concentration of Chl-*a* (0.6-1 mg m^{-3}) along the southern coast of Indonesian archipelago. In contrast with these conditions occur during northwest monsoon (NW) which is the positive SSHA (10-30 cm) following by warmer water of SST (28-30 ºC) and low concentration of Chl-*a* (0.1-0.5 mg m^{-3}) distributed at the same location along the southern coast of Indonesian archipelago. The EKE also showed a clear seasonal dependence with the SE monsoon give more favorable oceanographic conditions (500-2000 cm^2 s^{-2}) along the southern coast of Indonesian archipelago and in the offshore region around confluence of IOKW, SJC, RW and SEC around (11-16° S and 110-118° E). The maximum peaks of the favorable conditions correspond with the same months of SSHA, SST and Chl-*a* in the months of July and September but in the case of EKE continues to October until November overlapping with the early NW monsoon.

3. 2. Spatial and temporal patterns of the ocean variability

3. 2. 1. Empirical orthogonal function analysis

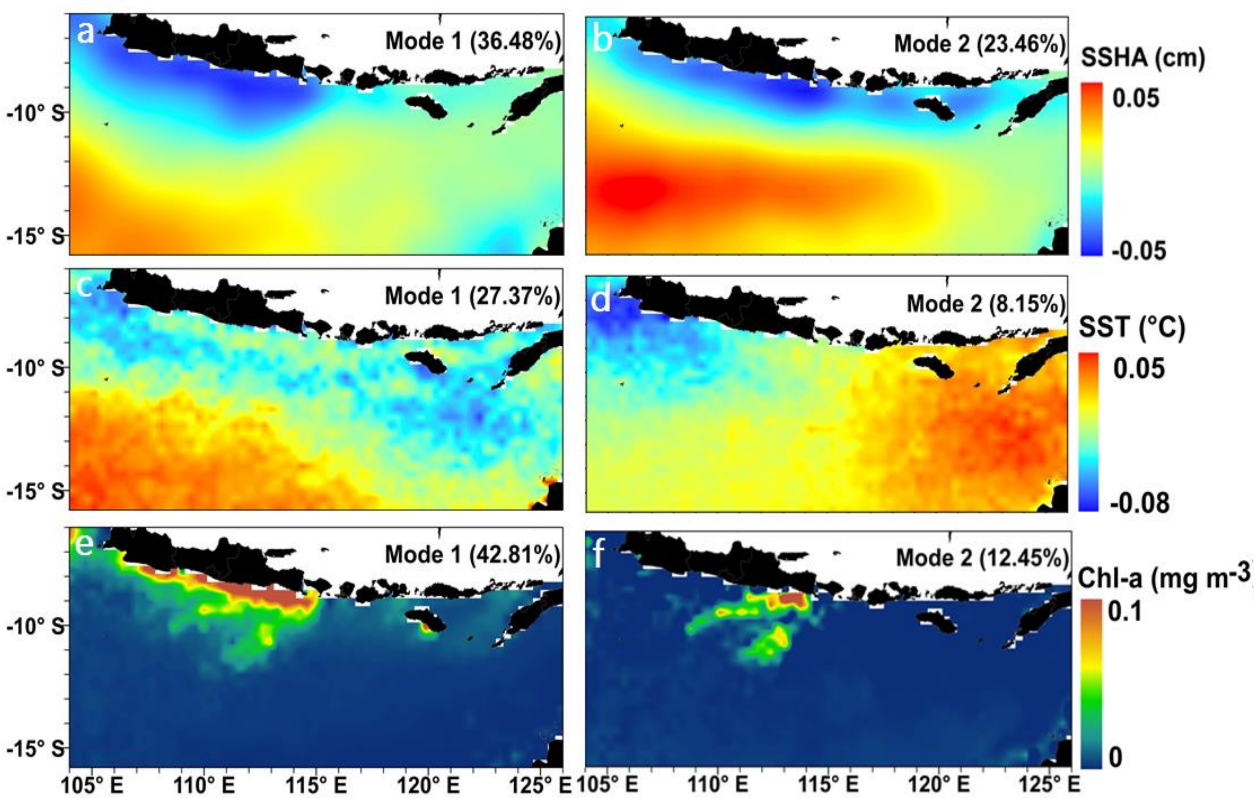

Figure 4. Spatial patterns of the EOF modes in the EIO off Java during 1997-2008: (a) first mode of SSHA, (b) second mode of SSHA, (c) first mode of SST, (d) second mode of SST, (e) first mode of Chl-*a*, (f) second mode of Chl-*a*. Scale units are in centimeters, degrees Celcius, and milligrams per cubic meter for SSHA, SST, and Chl-*a* data, respectively.

The spatial patterns of the first and second EOF modes of SSHA showed cold water to be located along the southern coast of Indonesian archipelago and warm water in the offshore region to make frontal areas along the latitudinal line of 10–12° S (Figure 4a and b). The first and second EOF modes contributed to 36.5% and 23.5% of total variances and corresponded to interannual and seasonal signals as indicated by the first and second temporal mode, respectively (Figure 5a and b).

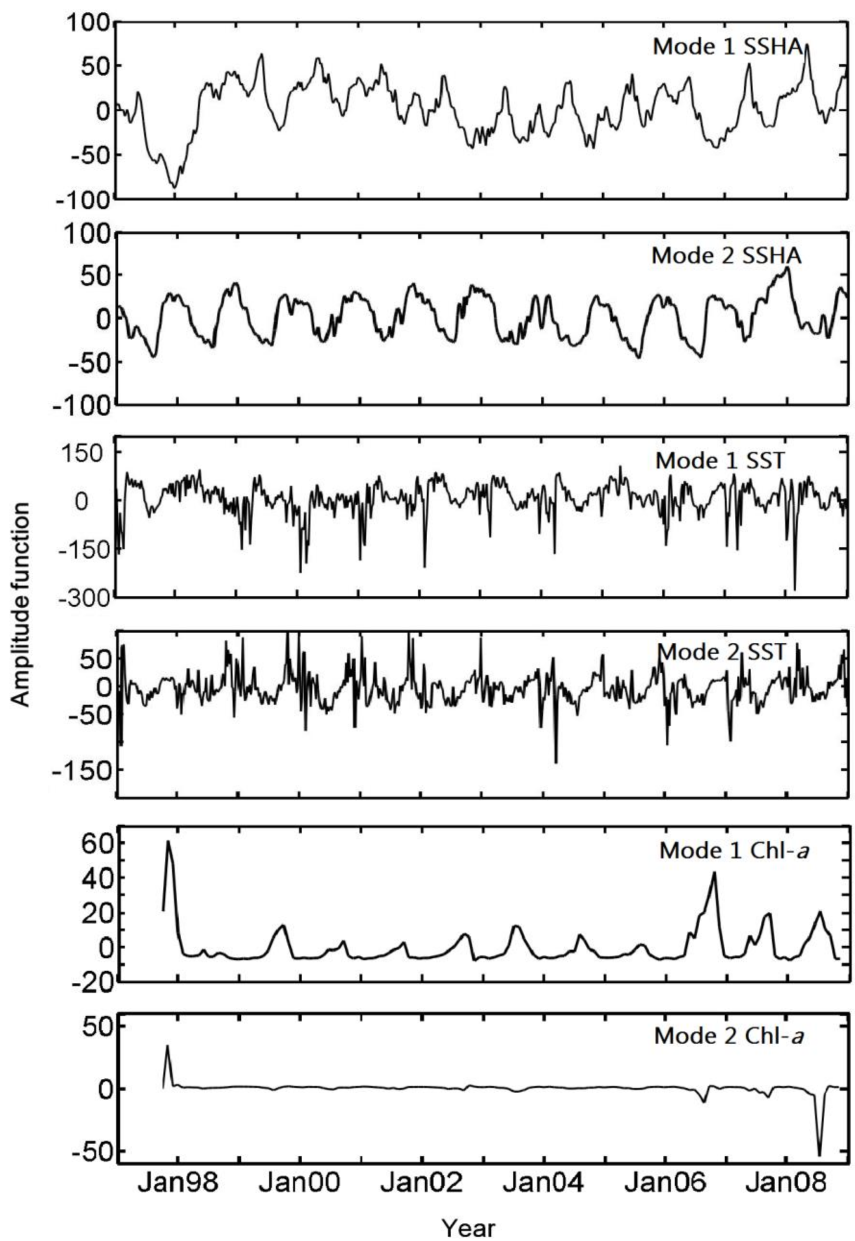

Figure 5. Amplitude function from the temporal mode of EOF analysis in the Southern Java Waters during 1997-2008: (a) first mode of SSHA, (b) second mode of SSHA, (c) first mode of SST, (d) second mode of SST, (e) first mode of Chl-*a*, (f) second mode of Chl-*a*. The x-axis represents year and the y-axis shows the amplitude function.

The spatial patterns of the first and second EOF modes of SST confirmed that the cold water found on the SSHA along the southern coast of Indonesian archipelago extended further to the offshore areas at 7-13° S to make the confluence region spread down south meeting with warm waters at 7-16° S and 117-125° E (Figure 4c and d). These EOF modes contributed to 27.4% and 8.2% of total variances and corresponded to interannual and seasonal signal for the first and second temporal modes, respectively (Figure 5c and d).

The spatial patterns of the first and second EOF modes of Chl-*a* clearly revealed a conduit high Chl-*a* concentration along the southern coast of Java and only distributed in the eastern tip of East Java waters, respectively (Figure 4e and f). These EOF modes contributed 42.8% and 12.5% of the total variances and corresponded to interannual and decadal signal for the first (Figure 5e and f) and second temporal modes, respectively. Total variances of the two major EOF modes of SSHA, SST and Chl-*a* accounted for 59.94%, 35.52%, and 55.26%, respectively (Table 2).

Table 2. Summary of the amplitude function (percentage of the total variability) of the first and second empirical orthogonal function modes of the sea-surface-height anomaly (SSHA), sea-surface temperature (SST), and chlorophyll-*a* (Chl-*a*) concentrations in the Southern Java Waters.

Parameter	Mode 1 (%)	Mode 2 (%)	Total (%)
SSHA	36.48	23.46	59.94
SST	27.37	8.15	35.52
Chlorophyll-*a*	42.81	12.45	55.26

The EOF analysis has been applied in the dominant mode forcing and its time scale variability on SSHA, SST, and Chl-*a*. The spatial patterns of the first and second EOF modes of SSHA, SST and Chl-*a* gave a very typical cold water of SSHA, low SST and high Chl-*a* concentration located along the southern coast of Indonesian archipelago and warm water of SSHA, high SST and much low Chl-*a* concentration in the offshore region to make frontal areas along the latitudinal line around 10–12 ºS. The frontal areas seemed to reveal the confluence region of IOKW and SJC that meet with the outflow of ITF from Lombok and Ombai straits and Timor passage and SEC.

The cold water, low SST and high Chl-*a* concentrations occurrence along the southern coast of Indonesian archipelago were likely a manifestation of El Niño and positive phase IOD events, and upwelling evidence as shown on the first and second EOF modes, respectively. These results are consistent with those Murtugudde et al. who investigated that in the Indian Ocean, intense warm events such as in 1997-1998 have direct impact on the primary production, the anomalous high values is observed in the Eastern Indian Ocean [13].

The EOF mode analysis for those oceanographic parameters infers that seasonal change has the strongest impact during the period of study from 1997-2008. Seasonal high Chl-*a* concentration along the southern coast of Java water occurred at coincident time with SST minimum (<28 °C) during the SE monsoon due to upwelling in this region and much low Chl-*a* concentration during the NW monsoon. This implied strong relationship for the seasonal change of SST and Chl-*a* along the southern coast of Java water [14, 15].

3. 2. 2. The wavelet spectrum analysis

The dominant periods related to the amplitude and phase time series were computed by the wavelet analysis. The wavelet analysis confirmed dominant signals related to amplitude (variance) and phases of SSHA, SST and Chl-*a* during 1997-2008 (Figure 6). The SSHA had also strong annual signal in particular during the 2001–2004 and 2006 periods, and semi-annual signal in 1999 and 2003 until 2005. Also, SST showed strong annual signal occurrence for the years 1999–2007 and semi-annual signal only during 1999–2000.

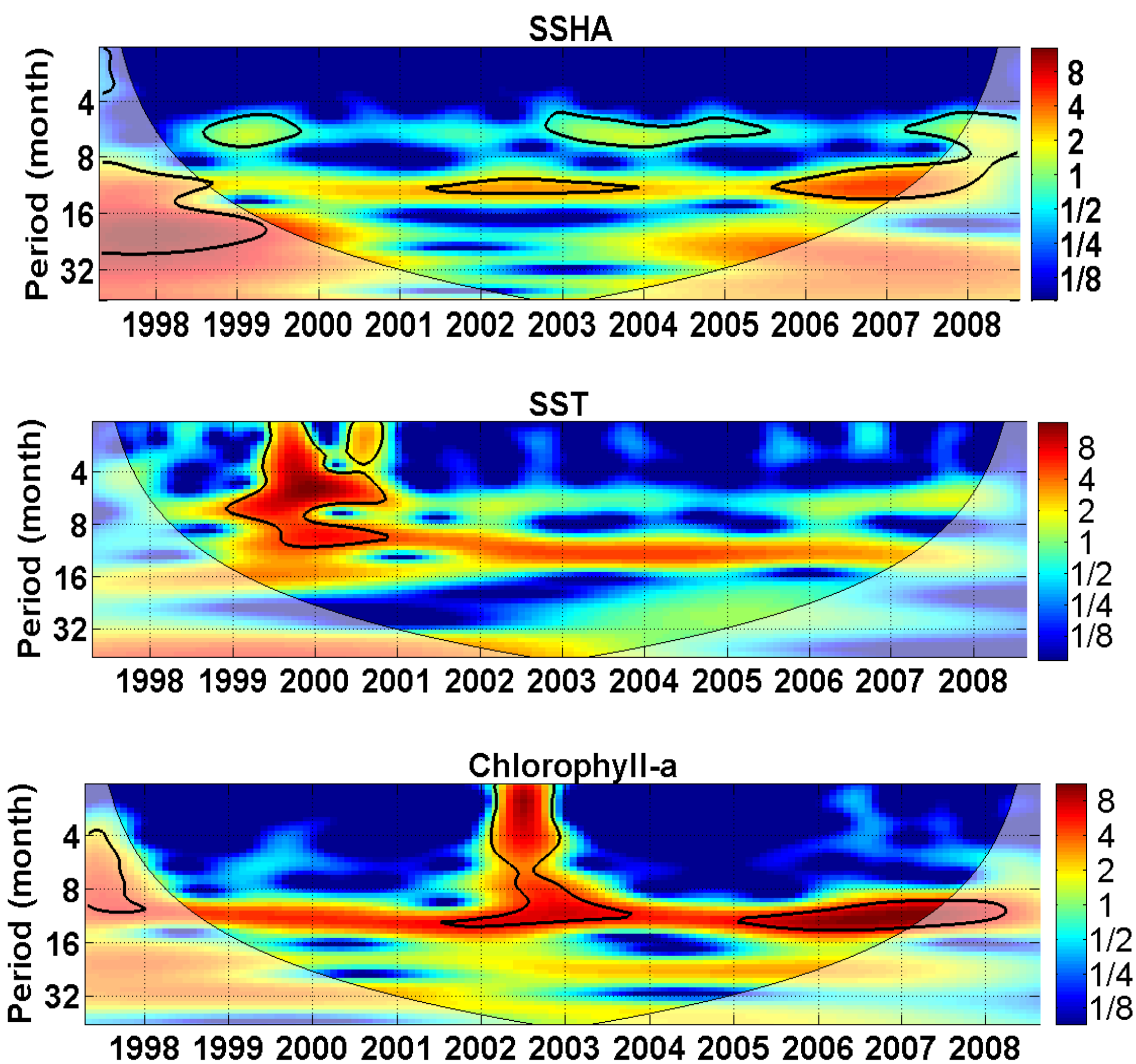

Figure 6. Wavelet power spectrum for SSHA, SST and Chl-*a* based on raw data (monthly mean) during 1997-2008. The y-axis is represented a period frequency (monthly) and x-axis showed the time (year). Colorbars represented different wavelet amplitude, the black line (solid contour) showed the 95% confidence level and a thin black line showed the cone of influence.

Similar strong annual signal along the year of 1999–2007 was observed in the Chl-*a* as well strong semi-annual signal only in 2002. It was interesting to note here that all parameters revealed strong annual signal in 1999–2007 with the strongest ones during 2001–2004 for SSHA. Semi-annual signal did not periodically occur to show strong signal in 2001–2002, 1999 and 2003–2005, 1999–2000, and 2000 for SSHA, SST and Chl-*a*, respectively. Furthermore, EOF and wavelet spectrum analysis provides evidence for the existence of the El Niño which clearly induced certain oceanographic conditions [16-18] in the Southern Java waters.

4. CONCLUSIONS

The results of this study have presented the influence of climate variability on the oceanographic conditions in the Southern Java Waters. It was interesting to note here that all parameters revealed strong annual signal in 1999–2007 with the strongest ones during 2001–2004 for SSHA. Semi-annual signal did not periodically occur to show strong signal in 2001–2002, 1999 and 2003–2005, 1999–2000, and 2000 for SSHA, SST and Chl-*a*, respectively.

The EOF modes further highlight that interannual and seasonal time scales are the main factors that affect ocean current variability in the study area. The EOF analysis also provides evidence for the effects of the 1997–98 El Niño event in the southern coast of Java, with the dominant features being negative SSHA, cold SST, and high Chl-*a* concentrations.

Acknowledgement

I wish to thank the Goddard Space Flight Center/NASA and Physical Oceanography Distributed Active Archive Center for the production of Chl-*a* and SST data, AVISO for the distribution of SSHA data, and the NOAA Climate Prediction Center for the use of its Niño 3.4 index and Japan Agency for Marine Earth Science and Technology (JAMSTEC) for the use of DMI index.

References

[1] O`Driscoll, K, A 3D regional model of the Indonesian Seas circulation. VDM Verlag Dr. Muller Aktiengesellschaft & Co, Sarbucken, Germany. (2008) 169p.

[2] Gordon, A. L, Oceanography of the Indonesian Seas and their throughflow. *Oceanography* 18 (2005) 13-26

[3] Saji, N. H., and T. Yamagata, Possible impacts of Indian Ocean Dipole mode events on global climate. *Climate Research* 25 (2003) 151-169

[4] Goelzer, H. A. Levermann and S. Rahmstorf, Two way coupling of an ENSO model to the global climate model CLIMBER-3α. *Ocean Modelling* 29 (2009) 94-101

[5] Lan, J., J. Hong., and Y. Wang. Relationship of the interannual variability of the Indonesian Throughflow with the IOD over the tropical Indian Ocean. *Theoretical and Applied Climatology* 97 (2008) 75-79

[6] Iizuka, S., T. Matsuura, and T. Yamagata, The Indian Ocean SST dipole simulated in a coupled general circulation model. *Geophysical Research Letters* 27(20) (2000) 3369-3372

[7] Susanto, R.D., A.L. Gordon, and Q. Zheng, Upwelling along the coasts of Java and Sumatra and its relation to ENSO. *Geophysical Research Letter* 28 (2001) 1599-1602

[8] Sprintall, J., S.E. Wijffel, R. Molcard, and I. Jaya, Direct estimates of the Indonesian Throughflow entering the Indian Ocean: 2004-2006. *Journal of Geophysical Research* 114 (2009) 1-19

[9] Polovina, J. J., and E.A. Howell, Ecosystem indicators derived from satellite remotely sensed oceanographic data for the North Pacific. *ICES Journal of Marine Science* 62 (2005) 319-327

[10] Kelly, K. A., Comment on "Empirical orthogonal function analysis of advanced very high resolution radiometer surface temperature patterns in Santa Barbara Channel" by G.S.E. Lagerloef and R.L. Bernstein. *Journal of Geophysical Research* 93 (1988) 15753-15754

[11] Menard F, F. Marsac, E. Bellier, and B Cazelles. Climatic oscillations and tuna catch rates in the Indian Ocean: a wavelet approach to time series analysis. *Fisheries Oceanography* 16 (2007) 95-104

[12] Torrence C, and G. P. Compo, A practical guide to wavelet analysis. *Bulletin of the American Meteorological Society* 79 (1998) 61-78

[13] Murtugudde, R. G., S.R. Signorini, J. R. Christian, A. J. Busalacchi, C. R. McClain, and J. Picaut, Ocean color variability of the tropical Indo-Pacific basin observed by SeaWiFS during 1997-1998. *Journal of Geophysical Research* 104 (1999) 18351-18366

[14] Qu, T., Y. Du, J. Strachan, G. Meyers, J. Slingo, Sea surface temperature and its variability in the Indonesian region. *Oceanography* 18 (2005) 50-123

[15] Susanto, R. D., and J. Marra, Effect of the 1997/1998 El Niño on Chl-*a* variability along the Southern Coasts of Java and Sumatera. *Oceanography* 18 (2005) 124-127

[16] Syamsuddin, M. L., Sunarto, L. P. Yuliadi and S. Harahap, Variability in fish catch rates associated with Sea Surface Temperature Anomaly (Nino 3.4 index) in the West of Java Sea. *World Scientific News* 117 (2019) 175-182.

[17] Achmad Rizal, Zuzy Anna, Climate Change and Its Possible Food Security Implications Toward Indonesian Marine and Fisheries. *World News of Natural Sciences* 22 (2019) 119-128

[18] Aastha Pudasainee, R. B. Ojha, Climate change: Policy and Politics. *World News of Natural Sciences* 13 (2017) 43-51